**Supplementary Information**

# Hot electron-driven hydrogen evolution using anisotropic gold nanostructure assembled monolayer $MoS_2$

Peng Zhang, Mamoru Fujitsuka, and Tetsuro Majima*

The Institute of Scientific and Industrial Research (SANKEN), Osaka University, Mihogaoka 8-1, Ibaraki, Osaka 567-0047, Japan

To whom correspondence should be addressed. E-mail: majima@sanken.osaka-u.ac.jp (T.M.).

## 1. Material synthesis

**Synthesis of Au nanoshere (Au NS).** The Au NS were synthesized by a seed-mediated method.[1] In the preparation of seed solution, a solution of 2.2 mM sodium citrate in Milli-Q water (150 mL) was heated with a heating mantle in a 250 mL three-necked round-bottomed flask for 15 min under vigorous stirring. A condenser was utilized to prevent the evaporation of the solvent. After boiling had commenced, 1 mL of $HAuCl_4$ (25 mM) was injected. The color of the solution changed from yellow to bluish gray and then to soft pink in 10 min. Immediately after the synthesis of the Au seeds and in the same reaction vessel, the reaction was cooled until the temperature of the solution reached 90 $^oC$. Then, 1 mL of a $HAuCl_4$ solution (25 mM) was injected. After 30 min, the reaction was finished. This process was repeated twice. After that, the sample was diluted by extracting 55 mL of sample and adding 53 mL of Milli-Q water and 2 mL of 60 mM sodium citrate. This solution was then used as a seed solution, and the process was repeated six times to obtain the required particle size.

**Synthesis of Au nanorod (Au NR).** Au NR were synthesized by a seed-mediated method.[2] Briefly, the seed solution was made by adding a freshly prepared, ice-cold aqueous solution of $NaBH_4$ (Sigma-Aldrich, 0.6 mL, 0.01 M) into a mixture solution consisting of $HAuCl_4 \cdot 3H_2O$ (Sigma-Aldrich, 0.025 mL, 0.1 M) and CTAB (TCI, 10

mL, 0.1 M). The solution was stirred vigorously for 2 min and aged at room temperature for 5 min before use. The growth solution was prepared by dissolving CTAB (9.0 g) and 5-bromosalicylic acid (Wako Pure Chemical Industries, 1.1 g) in 250 mL of warm water (Millipore, 55 $^{o}$C). To this solution, 4.8 mL of 0.01 M $AgNO_3$ (Sigma-Aldrich) was added, and after keeping undisturbed at room temperature for 15 min, 250 mL of 1 mM $HAuCl_4 \cdot 3H_2O$ solution was added. After gentle mixing of the solution for 15 min, 1.28 mL of 0.1 M freshly prepared ascorbic acid (Nacalai Tesque) was added with vigorously stirring for 30 s until the mixture became colorless. Then, 0.8 mL seed solution was added to the entire growth solution. The mixture was stirred for 30 s and left undisturbed at 27 $^{o}$C for 12 h and used in next step.

**Synthesis of Au nanotriangular (Au NT). T**he Au NT were synthesized by a seed-mediated method.[3] The initial seeds solution were prepared by the standard CTAC/$NaBH_4$ procedure: 25 μL of a 0.05 M $HAuCl_4$ solution was added to 4.7 mL of 0.1 M CTAC solution; 300 μL of a freshly prepared 0.01 M $NaBH_4$ solution was then injected under vigorous stirring. Excess borohydride was consumed by keeping the seed solution for 2 h at room temperature prior to use. In a typical synthesis of 40 mL of Au NT solution the following two growth solutions were prepared: (1) 1.6 mL of a 0.1 M CTAC solution was added to 8 mL of Milli-Q water, followed by 40 μL of 0.05 M $HAuCl_4$ solution and 15 μL of a 0.01 M NaI solution; (2) 500 μL of a 0.05 M $HAuCl_4$ solution was added to 40 mL of 0.05 M CTAC, followed by 300 μL of a 0.01 M NaI solution. The first solution was used to grow the CTAC capped seed into larger nanoparticles, while the second solution was used as the NT growth batch. Before proceeding, the initial seed@CTAC solution was diluted 10 × in a 0.1 M CTAC solution. Subsequently, 40 and 400 μL of 0.1 M AA solution were added to solutions 1 and 2, respectively, and both solutions were manually stirred until the complete transparency of the solutions was achieved, indicating Au III to Au I reduction. Finally, 100 μL of diluted seed@CTAC solution was added to solution 1 (and manually stirred for 1 s), and immediately 3.2 mL of this solution was added to solution 2 (and manually stirred for a few seconds). The Au NT dispersion was left undisturbed at room temperature for at least 1 h. It was observed that addition of 15

μL of a 0.01 M NaI solution to solution 1 further improved the yield in NTs obtained with the fast addition procedure. After spectroscopic characterization, the Au NT dispersion was purified by addition of a selected amount of 25 wt % CTAC solution. Flocculation of the Au NTs was completed overnight, the supernatant was then finally collected for further treatments.

**Preparation of $MoS_2$ nanosheets.** The lithium intercalation was carried out in a nitrogen-filled glovebox ([$O_2$] < 100 ppm). About 300 mg of bulk $MoS_2$ (Sigma-Aldrich) was immersed in 3 mL of *n*-butylithium and stirred for 2 days. The stock solution was filtered and washed with 100 mL hexane. Then the semi-dry powder was added in 300 mL of Milli-Q water and ultrasonicated for 1 h. The mixture was centrifugated and washed with Milli-Q water to remove the lithium cation and unexfoliated $MoS_2$.[4-6] It was eventually collected and redispersed in Milli-Q water (2 wt% CTAB). The concentration of $MoS_2$ in the suspension was determined as 10 mg $mL^{-1}$ by inductively coupled plasma (ICP) analysis.

**Preparation of Au nanostructures mono-assembled on $MoS_2$ nanosheets.** Followed high speed centrifugation and wash with 60 % $HClO_4$, 0.1 mL of Au solutions with different shapes was impregnated in 0.5 mL suspension of chemically exfoliated $MoS_2$ nanosheets under the continuously sonication for 30 min. Finally, the suspension was collected and redispersed in Milli-Q water (1 mg $mL^{-1}$).

**2. Characterizations.** The morphologies were investigated using scanning transmission electron microscopy (STEM) equipped with energy dispersive spectroscopy (EDS) mapping from JEM-ARM200F microscope operated at 200 kV. Extinction spectra were taken using quartz cuvettes of 1cm path length on a Shimadzu UV-3600 UV-VIS-NIR spectrophotometer. The concentration of Au nanostructures and $MoS_2$ were determined by ICP (Shimadzu, ICPS-8100).

**3. Photocatalytic $H_2$ generation tests.**

The aqueous suspensions of different shaped Au on $MoS_2$ layers were centrifuged at 12 000 rpm to remove excess surfactant and washed with Milli-Q ultrapure water for 2 times. The as-prepared catalysts were further treated with 60 % $HClO_4$ under ultrasonic condition for 10 min, then thoroughly washed and re-dispersed in

equivalent Milli-Q ultrapure water. 2 mL catalyst suspensions with 10 % lactic acid in 10 mL quartz cell was bubbled with Ar for 20 min, and sealed with a rubber septum. For visible-light hydrogen production, the suspensions were irradiated with visible-light (Asahi Spectra, LAX-C100; 200 mW $cm^{-2}$) with magnetic stirring at room temperature. A 460 nm cutoff filter was used to remove UV light. After the reaction, 0.1 mL of gas was collected from the headspace of the reactor and analyzed using a Shimadzu GC-8A gas chromatograph equipped with an MS-5A column and a thermal conductivity detector (TCD). To obtain an action spectrum, the irradiation of monochromated visible-nearinfrared light from the lamp equipped with different bandpass filters (Thorlabs, 10 nm fwhm) at different wavelengths was carried out.

**4. FDTD calculations.** The computational simulations were performed by using the finite-difference-time-domain (FDTD) method with perfectly matched layers (PML) boundary condition. A software package, FDTD Solutions 8.11 (Lumerical Solutions, Inc.), was employed to perform FDTD calculations. The optical constants of Au were adopted from tabulated values for bulk gold measured by Johnson and Christy.[7] The optical constants of 1T phase $MoS_2$ were introduced from reported data.[8] The Au NS is modeled as a sphere with a diameter of 57 nm. The Au NR is modeled as a cylinder with a length of 54 nm and a diameter of 14 nm. The Au NT is modeled as a triangular with a length of 57 nm and a thickness of 9 nm. The boundary with different shaped Au nanostructures inside was divided into meshes of 1 nm in size. For their dispersed in solutions, the refractive index of the medium was set to be 1.33 for water.

**5. Sample preparation for single-particle photoluminescence (PL) experiments.** The quartz cover glasses were purchased from Matsunami Glass and cleaned by sonication in a 20 % detergent solution (As One, Cleanace) for 6 h, followed by repeated washings with warm water for 5 times. Finally, the quartz cover glasses were washed again with Milli-Q ultrapure water (Millipore). The suspension of prepared Au with different shapes and their related composite were centrifuged at 12 000 rpm (Hitachi, himac CF16RX) to remove excess surfactant and washed with Milli-Q ultrapure water for 2 times. The final suspension with a low concentration were spin-

coated on the pre-cleaned quartz cover glass, which was subsequently annealed at 100 °C for 0.5 h to immobilize the particles on the glass surface.

**6. Single-particle PL measurements by confocal microscopy.** Single-particle PL images and spectra were recorded by using an objective scanning confocal fluorescence microscope system (PicoQuant, MicroTime 200). The samples were excited through an oil-immersion objective lens (Olympus, UplanSApochromat, 100×, 1.4 NA) with a circular-polarized 405 nm continuous wave (CW) laser controlled by a PDL-800B driver (PicoQuant). Typical excitation powers for the PL measurements were 300 μW at the sample. The emission from the sample was collected by the same objective and detected by a single-photon avalanche photodiode (Micro Photon Devices, PDM 50CT) through a dichroic beam splitter (Chroma, 405/488rdc) and long pass filter (Chroma, HQ513CP). For the spectroscopy, only the emission that passed through a slit entered the imaging spectrograph (Acton Research, SP-2356) that was equipped with an electron-multiplying charge-coupled device (EMCCD) camera (Princeton Instruments, ProEM).

**7. Time-resolved transient absorption measurements.** The femtosecond transient absorption spectra were measured by the pump and probe method using a regenerative amplified titanium sapphire laser (Spectra-Physics, Spitfire Pro F, 1 kHz) pumped by a Nd:YLF laser (Spectra-Physics, Empower 15). The seed pulse was generated by a titanium sapphire laser (Spectra-Physics, Mai Tai VFSJW; FWHM 80 fs). The output of the optical parametric amplifier (520 nm and 780 nm, 5 μJ $pulse^{-1}$, Spectra-Physics, OPA-800CF-1) was used as the excitation pulse. A white light continuum pulse, which was generated by focusing the residual of the fundamental light on a sapphire crystal after the computer controlled optical delay, was divided into two parts and used as the probe and the reference lights, of which the latter was used to compensate the laser fluctuation. Both probe and reference lights were directed to the sample and the transmitted lights were detected by a linear InGaAs array detector equipped with the polychromator (Solar, MS3504). The pump pulse was chopped by the mechanical chopper synchronized to one-half of the laser repetition rate, resulting in a pair of spectra with and without the pump, from which the absorption change (% absorption)

induced by the pump pulse was estimated. All measurements were carried out at room temperature.

**Supplementary Table 1. Lifetimes of Transient Absorption Decays.**

| Sample | Wavelength (nm) | $\tau_1 = \tau_3$ (ps) | $\tau_2 = \tau_4$ (ps) |
|---|---|---|---|
| $MoS_2$ | 600 | 23 | — |
| | 600 | 5.5 (76%) | 332 (24%) |
| AuNR | 735 | 5.9 (61%) | 327 (39%) |
| | 750 | 5.2 (61%) | 341 (39%) |
| | 600 | 5.4 (68%) | 222 (32%) |
| AuNR-$MoS_2$ | 705 | 5.6 (61%) | 756 (39%) |
| | 720 | 5.7 (52%) | 848 (48%) |

**Supplementary Figures**.

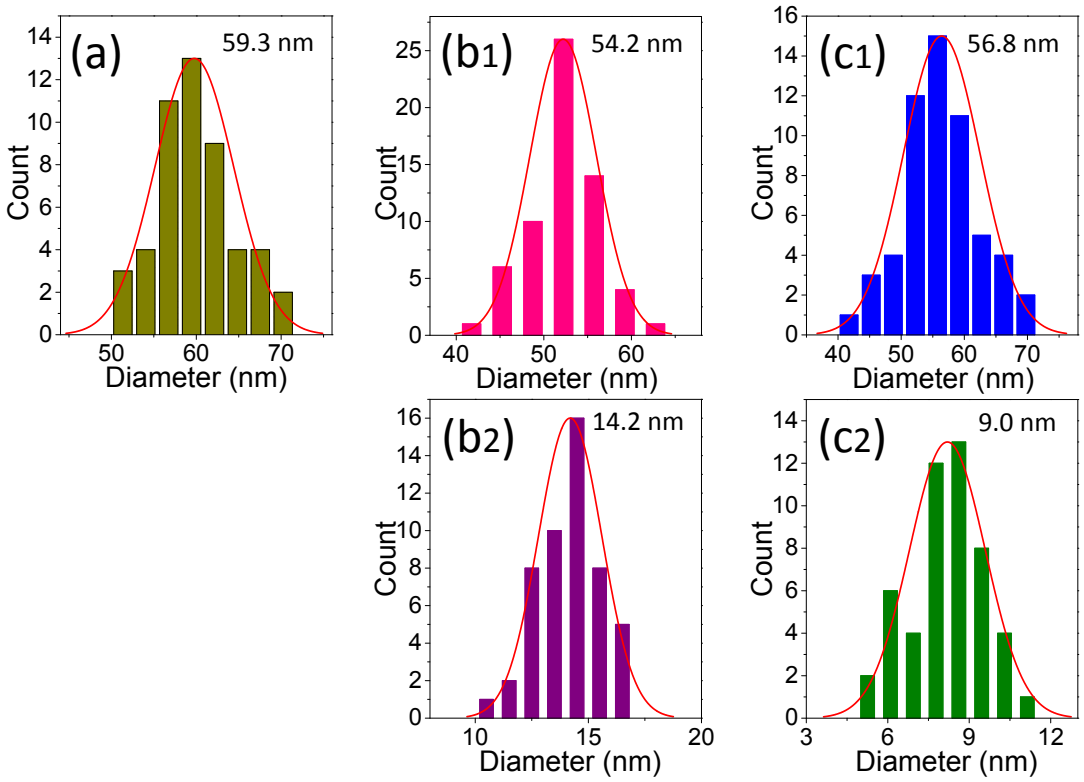


**Fig. S1** The size profiles of (a) AuNS, (b) AuNR, and (c) AuNT obtained from the corresponding TEM.

For the control experiments, we synthesized Au nanostructures with a few different sizes, i.e., AuNS with an average diameter of 55 ± 2 nm (Fig. S2, $a_1$) and 65 ± 2 nm (Fig. S2, $a_2$); AuNR with a length of 25 ± 3 nm and 34 ± 2 nm, and a similar diameter of 8 ± 1 nm and 8 ± 2 nm (Fig. S2, $b_1$ and $b_2$), respectively. The SPR wavelength was tailored by the size of nanostructures with a same shape. The SPR band of AuNS was observed at 523, 540, and 543 nm with the particle size of 55, 60, and 65 nm, respectively (Fig. S2, $a_3$). On the other hand, AuNR showed TSPR and LSPR peaks. TSPR peak did not show any shift, while LSPR peak was observed at 740, 754, and 810 nm for AuNR with the aspect ratio (length divided by width) of 3.1, 3.8, and 4.2, respectively (Fig. S2, $b_3$). Using these AuNS and AuNR with different sizes, a series of AuNS-$MoS_2$ and AuNR-$MoS_2$ were prepared to show the similar HER activity approximately 3 μmol $g^{-1}$ $h^{-1}$ and 14 μmol $g^{-1}$ $h^{-1}$, respectively. Therefore, the size changes of AuNS and AuNR in these ranges do not influence on the HER activity.

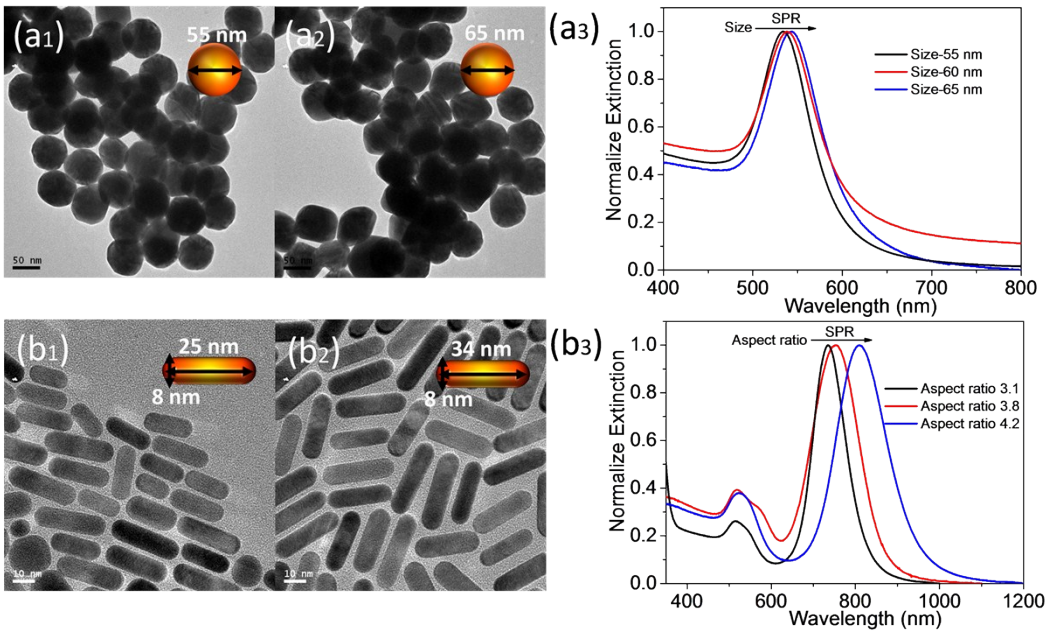


**Fig. S2** The aspect ratio dependent SPR wavelength of (a) AuNS and (b) AuNR obtained from the corresponding TEM.

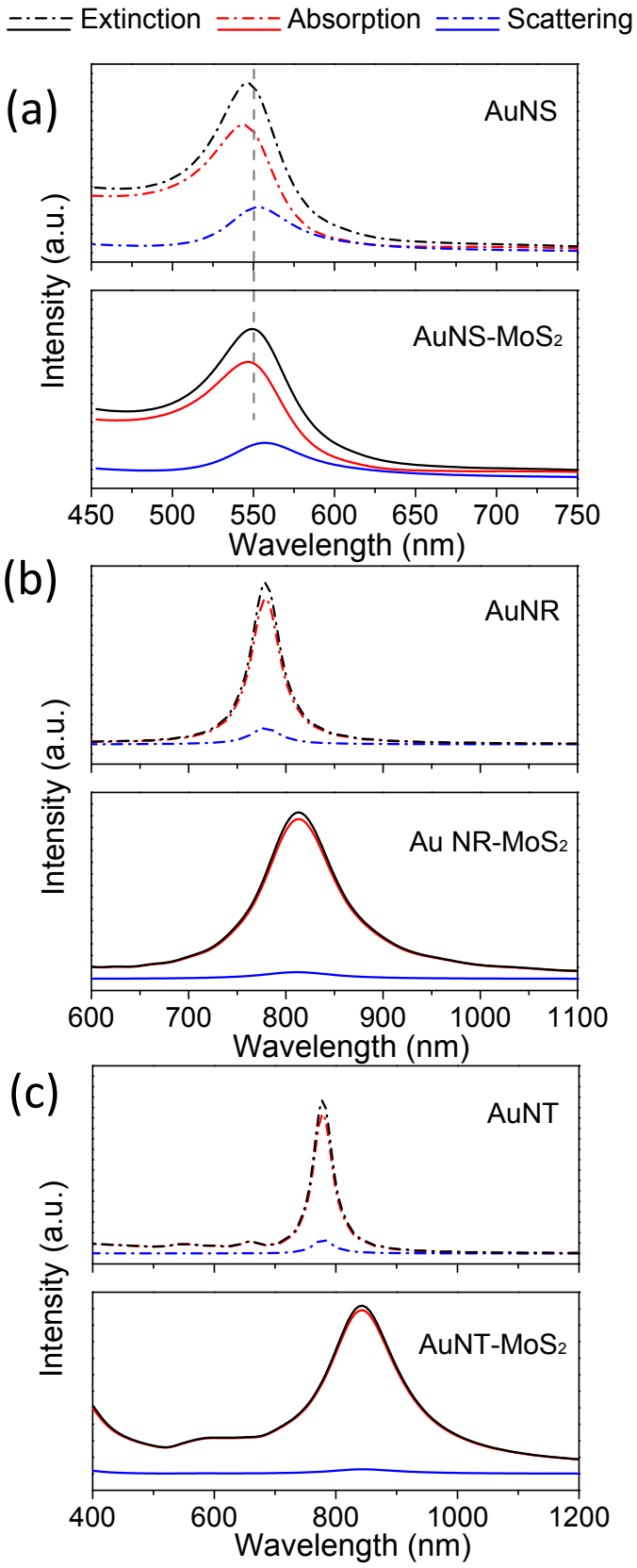


**Fig. S3** Calculated extinction spectra of (a) AuNS, (b) AuNR, and (c) AuNT and their corresponding composites assembled with $MoS_2$.

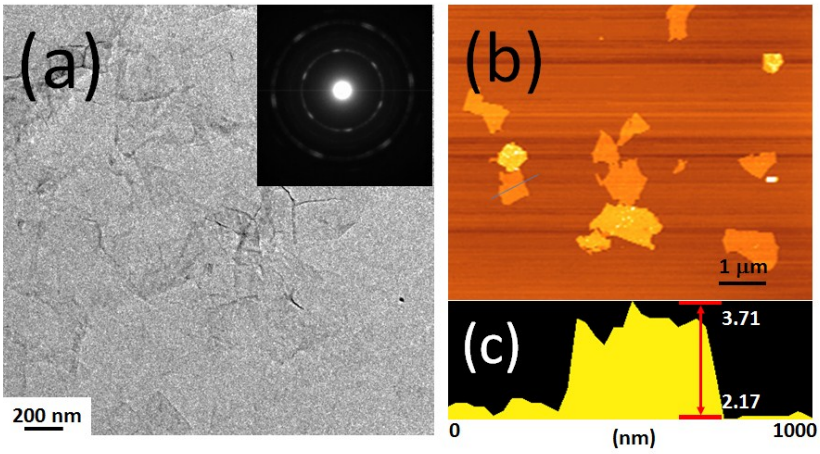


**Fig. S4** TEM image (a), AFM image (b) of $MoS_2$, and the height profile (c) of one nanosheet. The inset in panel (a) is the SAED pattern.

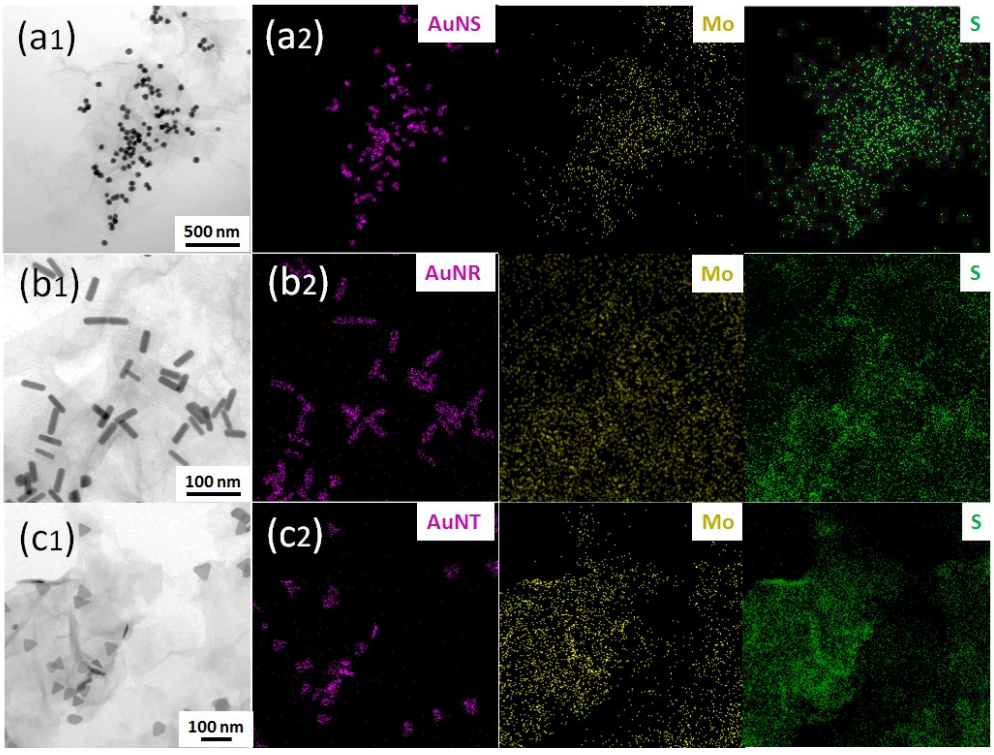


**Fig. S5** TEM images ($a_1$-$c_1$) and corresponding elemental mapping ($a_2$-$c_2$) of AuNS-$MoS_2$ (a), AuNR-$MoS_2$ (b), and AuNT-$MoS_2$ (c).

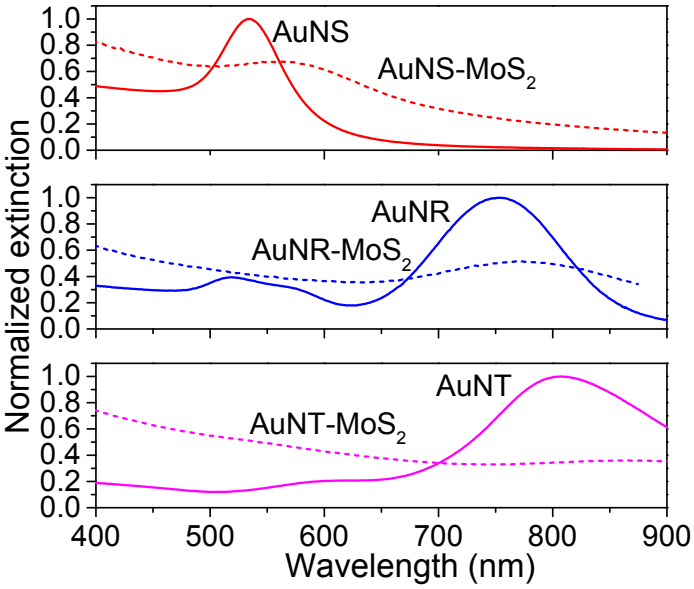


**Fig. S6** Comparison of peak shift and broadening between anisotropic Au and anisotropic Au nanostructures-$MoS_2$ from UV-vis-NIR extinction spectra.

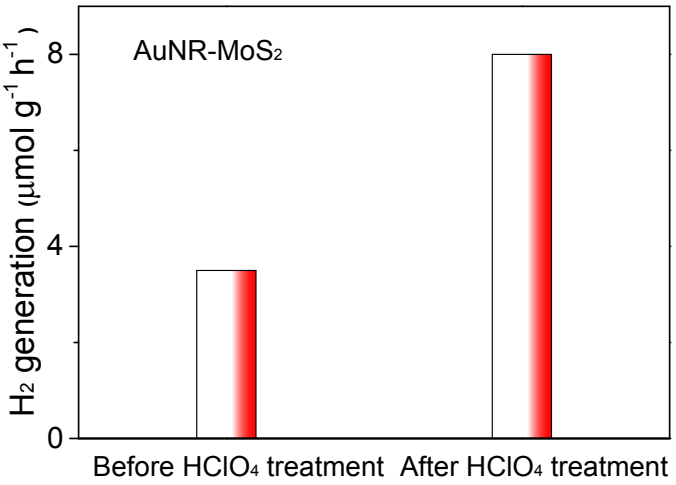


**Fig. S7** Comparison of the effect of $HClO_4$ treatment on $H_2$ evolution for AuNR-$MoS_2$.

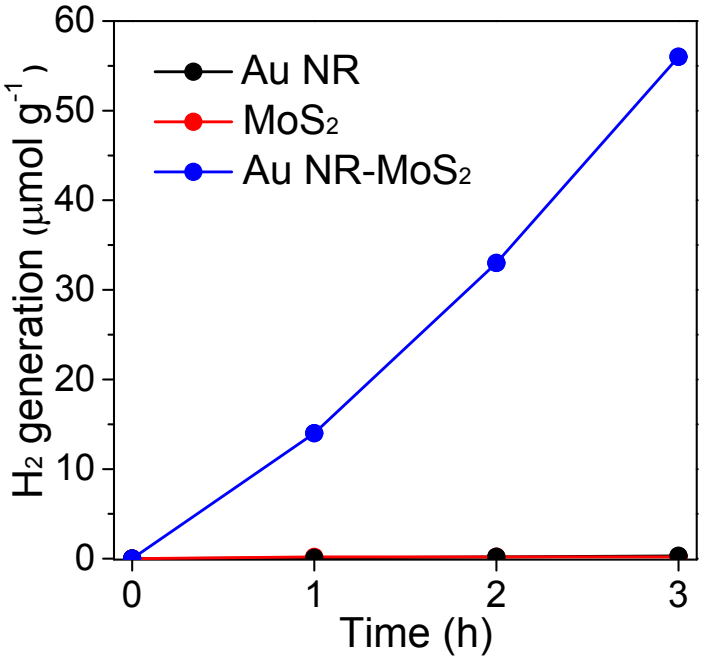


**Fig. S8** Comparison of $H_2$ evolution with pristine AuNR, $MoS_2$, and AuNR-$MoS_2$.

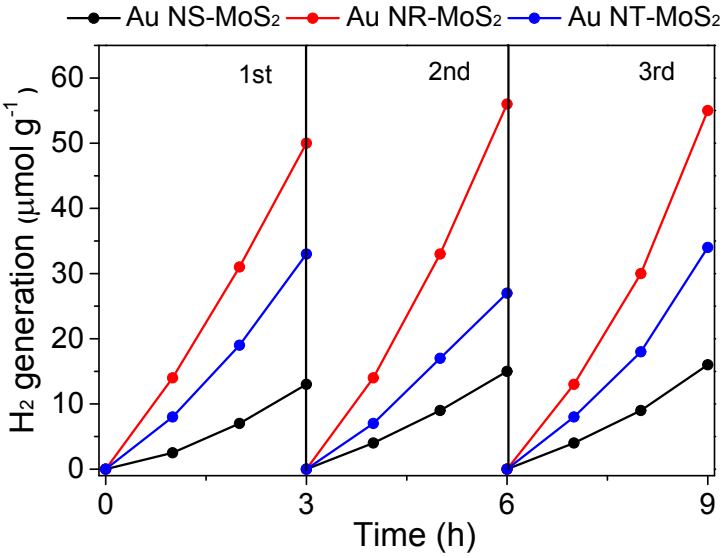


**Fig. S9** Repeated runs for $H_2$ evolution for AuNS-$MoS_2$, AuNR-$MoS_2$, and AuNT-$MoS_2$.

Both TSPR (~2.3 eV) and LSPR (~1.6 eV) bands can be excited simultaneously with the 520-nm excitation. The rapid interband absorption bleaching at 600 nm of AuNR-$MoS_2$ was similarly observed as with the LSPR band excitation at 780 nm arising from the interfacial hot electron injection from AuNR to $MoS_2$. However, the comparable amplitudes from AuNR and AuNR-$MoS_2$ are inconsistence between the transient and steady state spectra due to laser heating.[9]

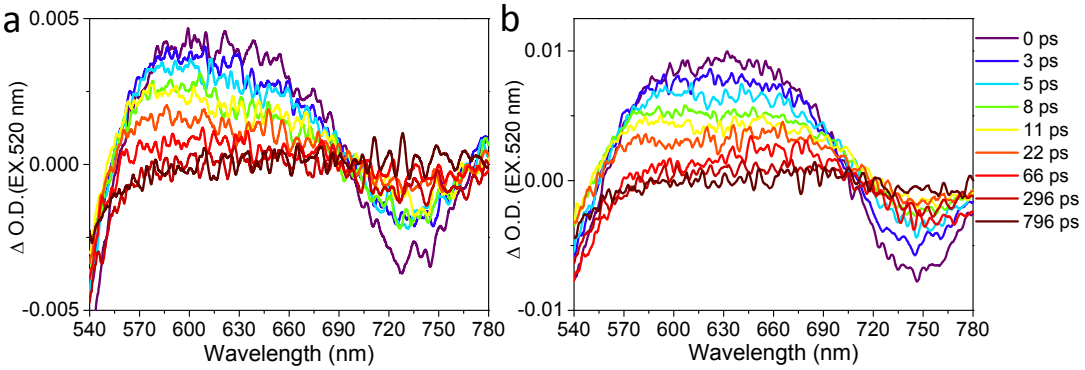


**Fig. S10.** Comparison of transient absorption spectra between the (a) AuNR and (b) AuNR-$MoS_2$ under the excitation at 520 nm.

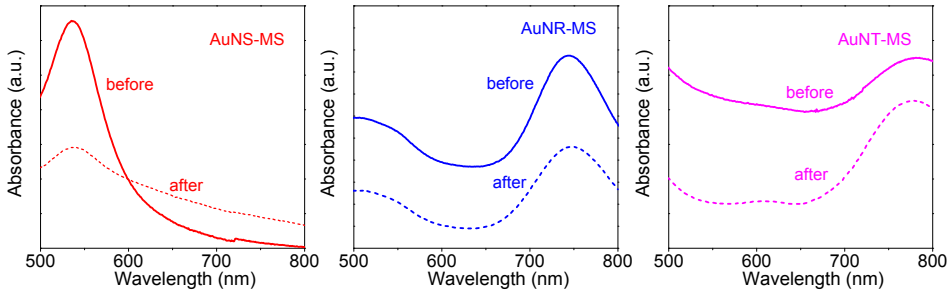


**Fig. S11.** Comparison of UV-vis-NIR extinction spectra from anisotropic Au nanostructures-$MoS_2$ before and after laser flash photolysis.

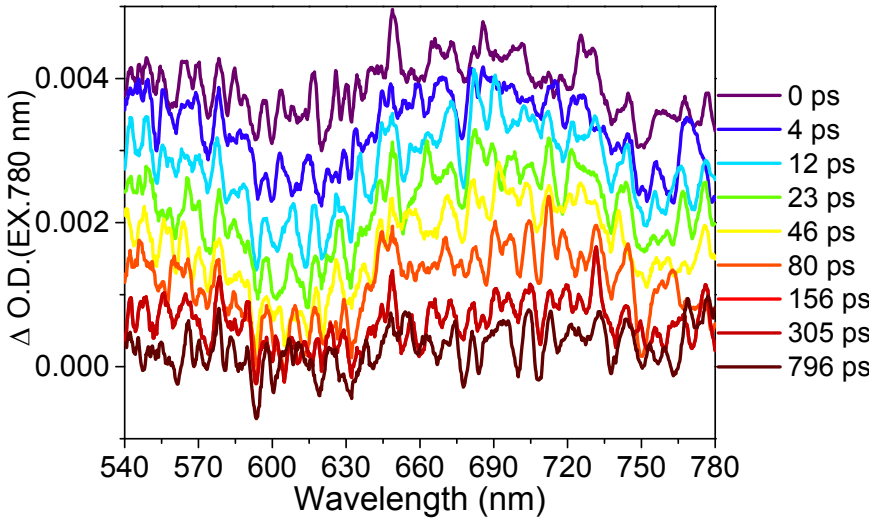


**Fig. S12.** The transient absorption spectra of $MoS_2$ with excitation at 780 nm.

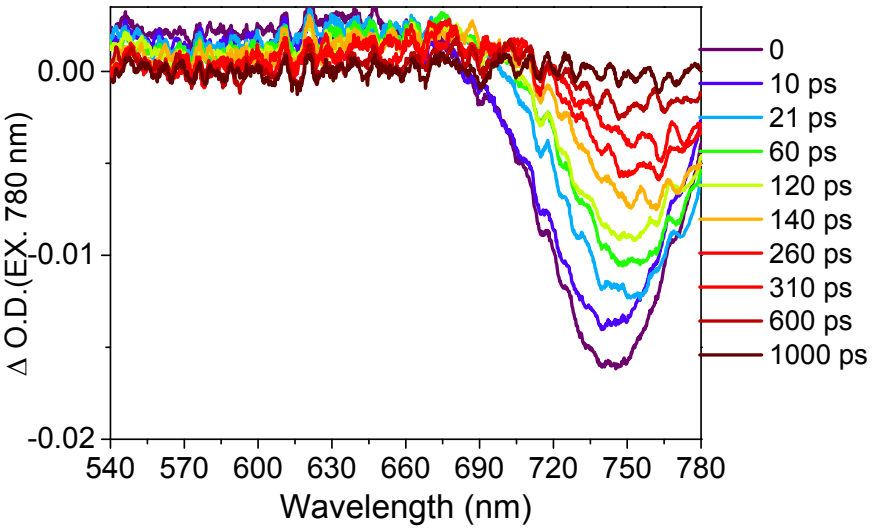


**Fig. S13.** The transient absorption spectra of AuNT-$MoS_2$ with excitation at 780 nm. The positive transient absorption in the range of 540-670 nm was observed to decay in the time scale of 0-800 ps, together with the bleaching and recovery of the LSPR band at 735 nm.

**References**


S1. N. G. Bastús, J. Comenge and V. Puntes, *Langmuir*, 2011, **27**, 11098-11105.

S2. Z. Zheng, T. Tachikawa and T. Majima, *J. Am. Chem. Soc.*, 2014, **136**, 6870-6873.

S3. L. Scarabelli, M. Coronado-Puchau, J. J. Giner-Casares, J. Langer and L. M. Liz-Marzán, *ACS Nano*, 2014, **8**, 5833-5842.

S4. G. Eda, H. Yamaguchi, D. Voiry, T. Fujita, M. Chen and M. Chhowalla, *Nano Lett.* 2011, **11**, 5111-5116.

S5. Y. Yu, S.-Y. Huang, Y. Li, S. N. Steinmann, W. Yang and L. Cao, *Nano Lett.*, 2014, **14**, 553-558.

S6. P. Zhang, T. Tachikawa, M. Fujitsuka and T. Majima, *Chem.Commun.*, 2015, **51**, 7187-7190.

S7. P. B. Johnson and R. W. Christy, *Phys. Rev. B*, 1972, **6**, 4370-4379.

S8. F. Xiong, H. Wang, X. Liu, J. Sun, M. Brongersma, E. Pop and Y. Cui, *Nano Lett.*, 2015, **15**, 6777-6784.

S9. S. Link, C. Burda, M. B. Mohamed, B. Nikoobakht and M. A. El-Sayed, *Phys. Rev. B*, 2000, **61**, 6086-6090.